Reverse polarity optical-OFDM (RPO-OFDM): dimming compatible OFDM for gigabit VLC links*

H. Elgala and T.D.C. Little
Multimedia Communications Laboratory
Department of Electrical and Computer Engineering
Boston University, Boston, Massachusetts
{*helgala, tdcl*}@*bu.edu*

July 08, 2013

MCL Technical Report No. 07-08-2013

Abstract– Visible light communications (VLC) technology permits the exploitation of light- emitting diode (LED) luminaries for simultaneous illumination and broadband wireless communication. Optical orthogonal frequency-division multiplexing (O-OFDM) is a promising modulation technique for VLC systems, in which the real-valued O-OFDM baseband signal is used to modulate the instantaneous power of the optical carrier to achieve gigabit data rates. However, a major design challenge that limits the commercialization of VLC is how to incorporate the industry-preferred pulse-width modulation (PWM) light dimming technique while maintaining a broadband and reliable communication link. In this work, a novel signal format, reverse polarity O-OFDM (RPO-OFDM), is proposed to combine the fast O-OFDM communication signal with the relatively slow PWM dimming signal, where both signals contribute to the effective LED brightness. The advantages of using RPO-OFDM include, (1) the data rate is not limited by the frequency of the PWM signal, (2) the LED dynamic range is fully utilized to minimize the nonlinear distortion of the O-OFDM communication signal, and (3) the bit-error performance is sustained over a large fraction of the luminaire dimming range. In addition, RPO-OFDM offers a practical approach to utilize off-the-shelf LED drivers. We show results of numerical simulations to study the trade-offs between the PWM duty cycle, average electrical O-OFDM signal power, radiated optical flux as well as human perceived light.

Keywords: Light-emitting diodes, optical communications, modulation, optical data processing, dimming control.

*In *Optics Express*, Vol. 21, Issue 20, pp. 24288-24299 (2013). This work is supported by the NSF under grant No. EEC-0812056. Any opinions, findings, and conclusions or recommendations expressed in this material are those of the author(s) and do not necessarily reflect the views of the National Science Foundation.

1 Introduction

Advances in solid-state lighting (SSL) are enabling LEDs to be the primary illumination source of the future [1]. The adoption of LEDs aims to significantly reduce energy consumption and facilitate precise intensity and color control of illuminated spaces [2]. Two methods are generally utilized to produce the white light in LED-based luminaries [3]. The cheapest and most popular is phosphor conversion, in which a blue LED is coated with phosphor to emit broad-spectrum white light. The second approach offers color-tunable lighting through combining monochromatic LEDs of different colors to produce white light through color mixing. Besides the several advantages of LEDs, they also have a fast response time making them excellent light sources for high-speed VLC links in which data is transmitted wirelessly from LED-based luminaries through subtle intensity variations [4]. In VLC systems, the communication signal is simply modulated onto the instantaneous power of the optical carrier and the optical detector generates a current proportional to the received instantaneous power, or intensity modulation with direct detection (IM/DD) [5]. VLC is motivated by several benefits including a huge, unregulated bandwidth (THz), license-free operation, no interference with RF systems, low-cost front-ends, and no health concerns, assuming compliance with eye safety regulations. Due to the potential synergy of indoor lighting and communication, it is unsurprising that VLC is gaining attention in academia and industry as a complementary to radio frequency (RF) technology [6] based on existing power-line infrastructure [7].

VLC research to date has primarily been focused on achieving increasingly high data rates [8, 9]. The spectrally-efficient O-OFDM is attractive to overcome the limited LED modulation bandwidth, thus constitutes a hot research topic in the field of VLC [10]. In O-OFDM based VLC systems, high data rates are supported through parallel transmission of high-order multilevel quadrature amplitude modulation (M-QAM) symbols on orthogonal sub-carriers. Assuming near-field communication in a static scenario, recent experimental setups have been demonstrated to achieve Gbps VLC links using commercial off-the-shelf components [11]. According to the laboratory conditions of these demonstrations, the human factors component and illumination features for a realistic illumination and communication system have been largely overlooked. Such research is vital to the adoption of VLC. For example, dimming is an essential feature in lighting to meet the functional and aesthetic requirements of a space as well as to conserve energy [12]. Additionally, a dimmed lamp produces less heat, extending the lifespan of LED light sources and reducing HVAC cooling loads. Paramount to the practical challenges of VLC is ensuring dimming functionality while maintaining a reliable broadband communication link. In the literature, to our knowledge, demonstrating the illumination compatibility with high-speed communication remains an open challenge.

Recent research efforts are conducted to assist in developing modulation techniques which address the challenge of incorporating broadband VLC with high-quality illumination and lighting state control. In [13], time-domain O-OFDM symbols are transmitted onto the PWM signal only during the ”on-state”. Here the data throughput is limited to the relatively low PWM line rate. In [14], the LED drive current is the time-domain O-OFDM signal multiplied by a periodic PWM pulse train. Here the practical communication is only feasible when the PWM signal is at least twice the frequency assigned to the largest O-OFDM sub-carrier frequency (*i.e.,* inter-carrier interference (ICI) for slower PWM rates). This constraint diminishes the feasibility of industry compatible dimmed broadband VLC link as PWM frequencies of off-the-shelf LED drivers are in

KHz.

In contrast, our work proposes a novel approach (1) to utilize the entire PWM cycle for data transmission instead of limiting the transmission to be only during the "on-state" so that the data throughput is not limited by the PWM frequency, (2) to use the full LED dynamic range of operation to minimize the nonlinear distortion (mainly clipping) of the O-OFDM signal and DC biasing is not required and the linear range of operation is extended, and (3) to maintain a high link capacity for a wide dimming range, and therefore, the signal-to-noise ratio (SNR) is independent on the dimming level within that wide range.

The remainder of this paper is organized as follows. PWM dimming and two versions of the O-OFDM baseband signal are highlighted in Section 2. The proposed RPO-OFDM is introduced in Section 3. In Section 4, the signal quality and perceived brightness are covered. The achieved system performance based on simulation results and relating to different system parameters is presented in Section 5. Conclusions are drawn in Section 6.

2 Dimming and O-OFDM modulation

Lighting controls can increase the value of buildings by making them more productive, comfortable, and energy efficient. This is often a product of dimming functionality that is application specific. For instance, settings such as conference rooms, office rooms or examination rooms, can require light levels as low as 1% percent of maximum illumination for aesthetic and comfort purposes. The brightness of an LED is adjusted by controlling the forward current through the LED. There are mainly two possible methods to dim LEDs: (1) analog dimming and (2) digital dimming. Analog dimming, also known as amplitude modulation (AM) or continuous current reduction (CCR), is the simplest type of dimming control. This technique lessens the current amplitude linearly to adjust the radiated optical flux. In digital dimming, the average duty cycle represents the equivalent analog dimming level. That is, a digitally modulated pulse train drives the LED at a constant current level. Pulse width modulation (PWM) is the simplest example of digital dimming modulation techniques. The time period of the PWM signal is fixed, whereas the duty cycle D varies proportionally to the required dimming percentage. Since PWM reduces light intensity more linearly than AM and induces less of a chromaticity shift, PWM is preferred in industry solutions [15].

A PWM signal current $i_{PWM}(t)$ with pulse width T and period T_{PWM} is shown in Fig. 1 and can be expressed as,

$$i_{PWM}(t) = \begin{cases} I_H, & 0 \leq t < T \\ I_L, & T < t \leq T_{PWM} \end{cases} \tag{1}$$

where I_H is the high level "on-state" LED current, I_L is the low level "off-state" LED current and $D = T/T_{PWM}$.

Asymmetrically clipped optical OFDM (ACO-OFDM) and DC biased optical OFDM (DCO-OFDM) are well known IM forms of O-OFDM [16]. Both are very similar to RF-OFDM, but they have their own requirements and methods. The Inverse Fast Fourier Transform (IFFT) operation modulates the O-OFDM sub-carriers and generates the time-domain signal. A real O-OFDM signal can be generated by constraining the input to the IFFT operation to have Hermitian symmetry ($S_n = S^*_{N-n}$). In ACO-OFDM, the generated bipolar signal is converted to unipolar through clipping of all negative values at zero. In DCO-OFDM, the generated bipolar time-domain signal

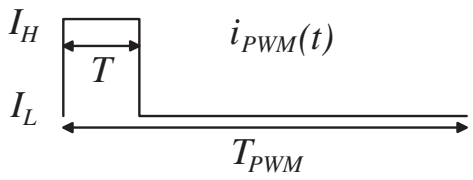

Figure 1: The PWM signal.

is used to modulate the optical carrier intensity after DC biasing of the LED. To demonstrate the proposed approach, the ACO-OFDM signal format is considered. The generated time-domain ACO-OFDM current samples and signal current can be mathematically described as follows:

$$i_k = \sum_{n=0}^{N-1} S_n \exp^{\left(j\frac{2\pi}{N}nk\right)} \tag{2}$$

$$i_{OFDM}(t) = \sum_{n=0}^{N-1} S_n \exp^{(j\omega_n t)}, 0 \leq t < T_{OFDM} \tag{3}$$

where, the values $S_n, n = 0, \cdots, N-1$ are the input data symbols of the n^{th} sub-carrier, $i_k, k = 0, \cdots, N-1$ are the N time-domain output current samples, $i_{OFDM}(t)$ is the O-OFDM time-domain signal current, T_{OFDM} is the time-domain O-OFDM symbol period, and $\omega_n = 2\pi n/T_{OFDM}$. A normalized ACO-OFDM time-domain symbol is also shown in Fig. 2.

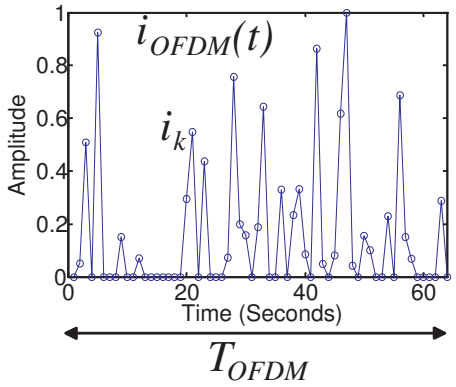

Figure 2: The unipolar ACO-OFDM symbol. The circles represent the different current samples of the ACO-OFDM symbol and the solid blue line represents the analog ACO-OFDM signal current ($i_{OFDM}(t)$) after a digital-to-analog conversion.

Unsurprisingly, dimming presents a number of immediate challenges to VLC. By its very nature, dimming reduces the average signal strength. It also places extra constraints on the O-OFDM modulation scheme which must enable both data transmission and light intensity adjustment. In the context of these problems, an intensity control approach is proposed to achieve optimal data rates without sacrificing illumination features as well as quality.

3 The proposed RPO-OFDM

In this work, it is proposed to combine $i_{OFDM}(t)$ with $i_{PWM}(t)$ as follows:

$$i_{LED}(t) = \begin{cases} i_{PWM}(t) - m \times i_{OFDM}(t), & 0 \leq t \leq T \\ i_{PWM}(t) + m \times i_{OFDM}(t), & T < t \leq T_{PWM} \end{cases} \tag{4}$$

where, $i_{LED}(t)$ is the LED drive current and m is a real-valued scaling factor of the O-OFDM modulating signal that sets the average electrical O-OFDM signal power P_{OFDM}.

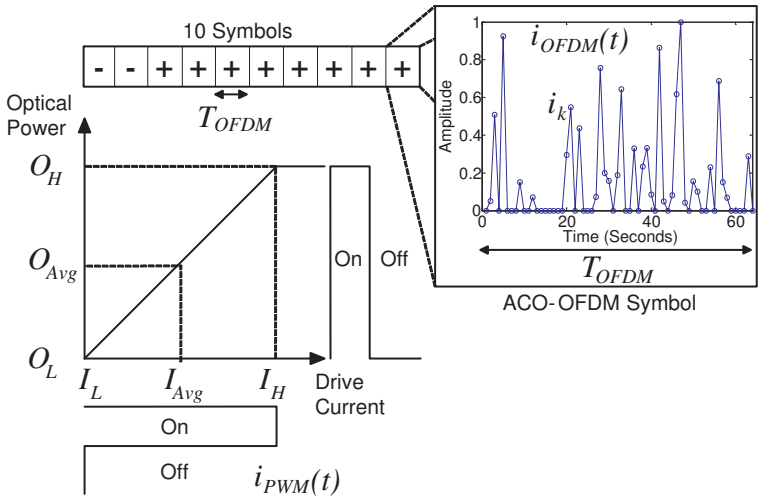

Figure 3: An example to demonstrate the proposed RPO-OFDM system: based on the dimming level, D, the polarity of the O-OFDM symbols are adjusted before the O-OFDM signal is superimposed on the PWM signal. The non-linear transfer function of the LED: O_L denotes the output optical power corresponding to the input current I_L and O_H denotes the output optical power corresponding to the input current I_H.

The LED non-linear transfer function and the proposed system with an example are illustrated in Fig. 3. The non-linear transfer function relates the input LED drive current to the output optical power. The emitted optical power of a $i_{PWM}(t)$ pulsating between I_L and I_H is shown. I_H is assumed to correspond to the maximum allowed $i_{LED}(t)$ and I_L corresponds to the minimum $i_{LED}(t)$ according to the LED data sheet. The LED dynamic range can be denoted by I_H-I_L. In the proposed system, $i_{OFDM}(t)$ is superimposed on $i_{PWM}(t)$ after setting a proper polarity of the individual ACO-OFDM symbols using a RPO-OFDM modulator depending on whether the symbol is being transmitted on I_H or I_L during T_{PWM}. To explain the idea of RPO-OFDM with an example, $D = 20\%$, 10 ACO-OFDM symbols, $i_k = 64$ and $T_{PWM} = 10 \times T_{OFDM}$ are assumed. Consequently, the polarity of the first two ACO-OFDM symbols is reversed (-ve polarity), then transmitted on the I_H followed by 8 ACO-OFDM symbols (+ve polarity), transmitted on I_L. At the receiver side, and after time-synchronization, all 640 samples are extracted and the polarity of the first 128 samples is re-adjusted. Figure 4 shows ACO-OFDM symbols that are sequentially transmitted at $D = 20\%$ and $D = 70\%$.

The building blocks of the RPO-OFDM modulator are shown in Fig. 5. The serial data bits are grouped into symbols and modulated using a QAM modulator. The mapper assigns the symbols to

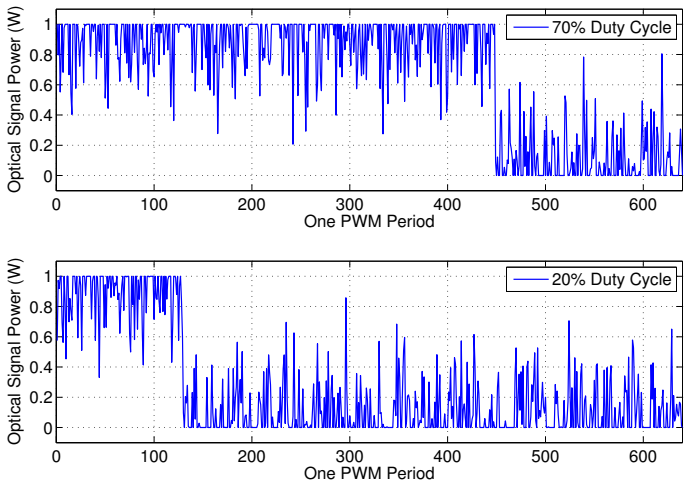

Figure 4: Optical RPO-OFDM signal waveform based on ACO-OFDM at 70% D (upper) and 20% D (lower). $I_H = 1A$, $I_L = 0A$, 8-QAM and $P_{OFDM} = 16dBm$.

the IFFT input bins (sub-carriers). The O-OFDM symbol is assembled in frequency domain and the O-OFDM time domain signal is obtained using the IFFT operation. Based on how the symbols are assigned to the sub-carriers, the unipolar operation forms unipolar O-OFDM symbols such as the operation used to generate the ACO-OFDM [16], the Flip-OFDM [17], the position modulation OFDM (PM-OFDM) [18] or the unipolar OFDM (U-OFDM) [19]. A fixed length cyclic prefix (CP) (to avoid any inter-symbol interference (ISI)) is added before the polarity inverter. Based on the target dimming level, D, the polarity inverter is activated.

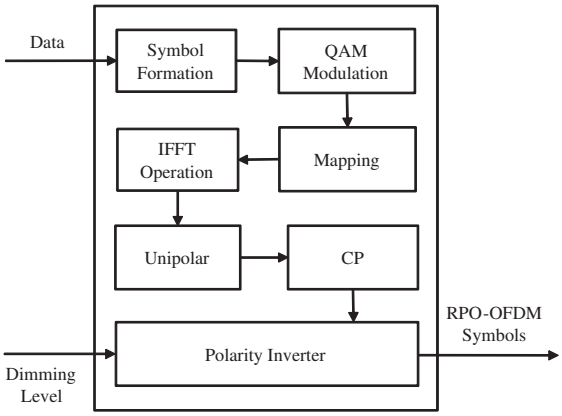

Figure 5: Building blocks of the RPO-OFDM generator.

As shown in Fig. 6(a), the proposed approach considers, for example, modulating the dimming signal current $i_{PWM}(t)$ supplied by the LED driver (assuming PWM as shown in Fig. 6(b)) using the polarity-adjusted O-OFDM analog signal current ($i_{OFDM}(t)$) available after the RPO-OFDM modulator according to a dimming set point D. There are different circuit topologies to combine $i_{PWM}(t)$ and $i_{OFDM}(t)$ to obtain $i_{LED}(t)$. It is also possible to realize a circuit topology to directly

drive the LED using $i_{OFDM}(t)$ (see Fig. 6(c)). However, these topics are not the scope of the paper and will be shown in a latter work. It is also worth pointing out that RPO-OFDM can also be applied to any unipolar O-OFDM version or the bipolar O-OFDM version (*e.g.,* DCO-OFDM). For example, the same modulation-demodulation sequence is valid for a bipolar DCO-OFDM, however using two consecutive PWM periods.

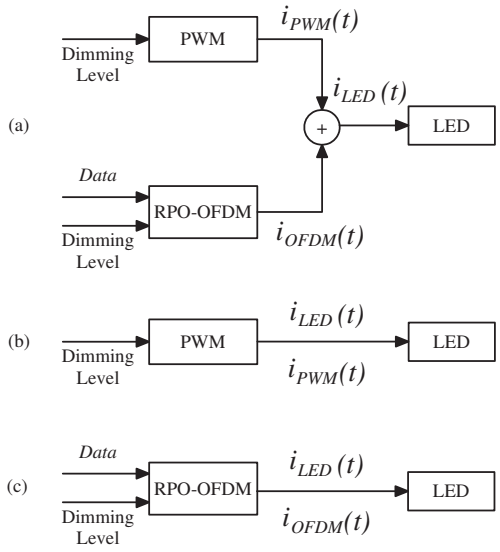

Figure 6: (a) modulating the dimming signal current $i_{PWM}(t)$ using the polarity-adjusted O-OFDM analog signal current $i_{OFDM}(t)$. (b) PWM dimming without RPO-OFDM VLC. (c) directly drive the LED using $i_{OFDM}(t)$.

4 Signal quality and perceived brightness

In terms of spectral efficiency and bit-error performance, the proposed approach based on PWM offers several advantages over AM. Using AM, the ACO-OFDM signal is superimposed on a fixed bias level. The consequences are reduced LED dynamic range for transmission, the ACO-OFDM signal power has to be optimized for each bias level and the performance is directly relate to the dimming set-point. However, in the proposed approach, and assuming that the PWM signal is utilizing the full LED dynamic range, the ACO-OFDM signal clipping is avoided for a wider amplitude-range of OFDM samples and the transmitted OFDM signal shape is preserved. Preserving the OFDM signal shape corresponds to less induced clipping noise allowing the use of high-order constellations (better spectral efficiency) or the establishment of more robust links (better BER). The proposed approach decouples dimming for a wide-range from the performance, and assuming optimum ACO-OFDM signal power to maintain a target quality of service (QoS).

The SNR for each scaled ACO-OFDM symbol is the ratio between the power of the undistorted part of the signal and noise power and can be expressed as,

$$SNR \propto \frac{\sigma_{LED}^2}{\sigma_N^2} \propto \frac{m^2 \sigma_{OFDM}^2}{\sigma_N^2} \tag{5}$$

where, σ^2_{LED} denotes the LED current variance and σ^2_N denotes variance of the additive white Gaussian noise (AWGN) representing shot and thermal noise. Any DC optical power component or increase in D does not contribute to SNR improvement. The SNR can be improved only through maximizing σ^2_{LED}/ and maximum P_{OFDM} being determined by the value of the scaling factor m. However, to ensure that i_k stays within the dynamic range of the LED, a maximum m with absolute value of $I_H/max(i_k)$ is required. At a certain P_{OFDM}, If the magnitude of any i_k sample is beyond the dynamic range of the LED, and assuming $I_L = 0$, $i_{LED}(t)$ will be clipped and the clipped signal $i'_{LED}(t)$ is given by

$$i'_{LED}(t) = \begin{cases} 0, & i_k \geq I_H \text{ (on-state)} \\ i_{LED}(t), & i_k < I_H \\ I_H, & i_k \geq I_H \text{ (off-state)} \end{cases} \tag{6}$$

For such clipped signal, the SNR is calculated again using the ratio between the power of the undistorted part of the signal and the effective noise power, which now accounts for contributions caused by shot and thermal noise as well as induced clipping noise.

As shown previously in Fig. 3, the average optical power denoted by O_{Avg} can be controlled by adjusting D or jointly adjusting D and m. An optimum m is determined based on the available LED dynamic range, the target dimming range and the M-QAM order. Over one PWM period, O_{Avg} corresponds to an average LED current denoted by I_{Avg} and described as,

$$I_{Avg} = D(I_H - \frac{mi}{N}\sum_{k=0}^{N-1} i_k) + (1-D)(I_L + \frac{mj}{N}\sum_{k=0}^{N-1} i_k) \tag{7}$$

where, i is the number of the O-OFDM symbols transmitted during the "on-state" and j is the number of the O-OFDM symbols transmitted during the "off-state". Assuming the LED input-output characteristic as shown in Fig. 3, $I_L = 0$ and $D = 50\%$, it is clearly observed that I_{Avg} is always equal to half the I_H and independent on m, (*i.e.* P_{OFDM}).

As for brightness, the human eye responds to lower O_{Avg} by enlarging the pupil, allowing more light to enter the eye. This response results in a non-linear relation between measured and perceived light levels that is captured by the following formula:

$$Perceived\,Light\,(\%) = 100 * \sqrt{\frac{Measured\,Light\,(\%)}{100}} \tag{8}$$

5 Simulation results

Simulations are conducted to investigate the influence of D and P_{OFDM} on the radiated optical power and optical dimming, as well as the perceived LED brightness and dimming. The dimming level is defined as a percentage of the maximum brightness where 100% dimming is full brightness. $I_H = 1A$, $I_L = 0A$ and P_{OFDM} are calculated over one ACO-OFDM symbol. Modulating signal current values above 1A are clipped. Figure 7 shows the obtained optical dimming and perceived dimming as a function of D. Curves are obtained at different values of P_{OFDM} that is incremented starting 10dBm up to 24dBm in steps of 2dBm. The numerical results confirm that the optical dimming can be linearly adjusted by varying D for different values of P_{OFDM}. The O-OFDM signal is the sum of N independent sub-carriers. For large values of N (N>10), the ACO-OFDM

envelope can be accurately modeled as a Gaussian random process (due to the central limit theorem) with zero mean. Thus at $D = 50\%$, P_{OFDM} has no effect on the dimming level. It is also highlighted that the human eye has better sensitivity at low luminance than high luminance. The non-linear relation between optical dimming and perceived dimming is clearly observed. For instance, decreasing the optical power by 50% achieves only a 70% reduction in brightness.

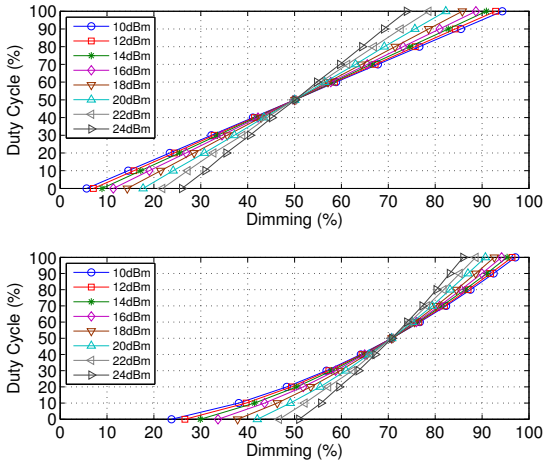

Figure 7: Optical dimming (upper) and perceived dimming (lower) as a function of D and P_{OFDM}.

Figure 8 illustrates how the dimming range decreases as P_{OFDM} increases. At any P_{OFDM} value, the range between the two vertical circles represents the optical dimming range, however the range between the two vertical squares represents the perceived dimming range. For low P_{OFDM}, (*e.g.* at $P_{OFDM} = 10dBm$), the full dimming range is slightly reduced by 10%, from 95% up to 5%. At $P_{OFDM} = 16dBm$, the highest brightness level that can be achieved is limited to 90% and the highest dimming level that can be reached is 10%. Further increase of P_{OFDM} narrows the dimming range around 50% dimming.

The influence of P_{OFDM} on the system bit-error performance is also investigated. In these Monte-carlo simulations, un-coded 8-QAM, 16-QAM, and 32-QAM modulation schemes, -3dBm AWGN, $I_H = 1A$, $I_L = 0A$ and perfect synchronization between the transmitter and the receiver are assumed. Typical receiver sensitivity is around -30dBm, however a high AWGN value of -3dBm, is chosen in order to be able to illustrate the full behavior of the bit-error ratio (BER) curves and to avoid BER values below 10^{-6} that are difficult to obtain using simulations. For a target BER of 10^{-3}, it is clearly confirmed that for all three curves, $P_{OFDM} = 10dBm$ is not sufficient to achieve the target BER. Above 14dBm and below 21dBm, 8-QAM and 16-QAM curves show BER values better than 10^{-3}. However, for wider dimming range $P_s = 14dBm$ is recommended as illustrated in Fig. 8. To achieve BER of 10^{-3} using 32-QAM, P_{OFDM} must be set at 18dBm. The SNR and BER are improved, as expected, with the increase of P_{OFDM} reaching an optimal value for a specific noise power. By further increasing P_{OFDM}, the SNR starts to deteriorate as a result of induced non-linear distortions caused by the LED limited dynamic range (clipping at 1A). AWGN noise dominates at low P_{OFDM} values and clipping distortion dominates at high P_{OFDM} values. The optimum P_{OFDM} values for 8-QAM, 16-QAM, and 32-QAM are 16dBm, 17dBm and 18dBm, respectively.

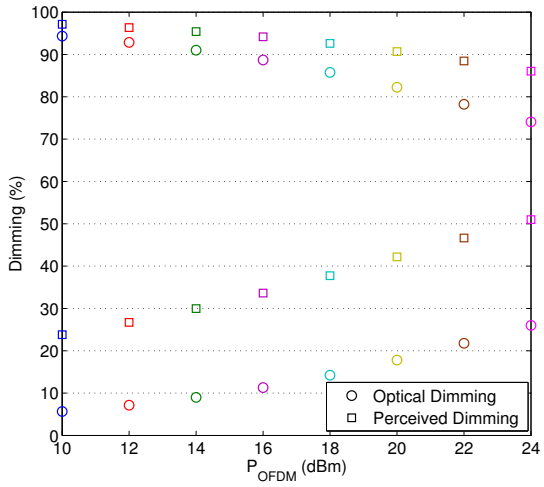

Figure 8: The influence of P_{OFDM} on the achieved optical dimming and perceived dimming ranges.

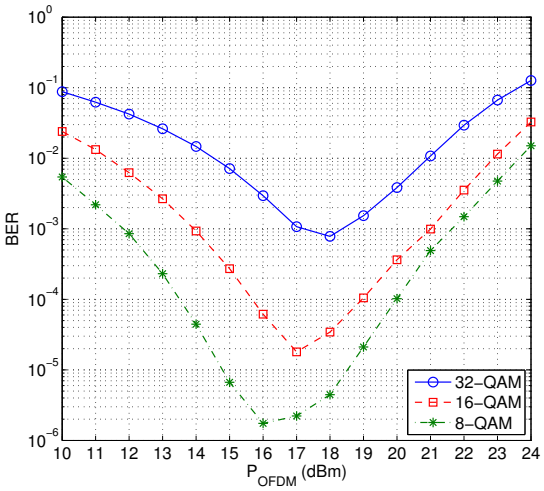

Figure 9: Bit-error performance as a function of P_{OFDM} for un-coded 8-QAM, 16-QAM, and 32-QAM modulation schemes.

A VLC enabled lighting design must carefully consider to meet the challenge of providing a lighting plan that acknowledges the unique qualities and services of individual spaces and applications. Using Fig. 8 and Fig. 9 (having the same x-axis), for example, at 8-QAM, the lowest BER of 10^{-6} is achieved at $P_{OFDM} = 16dBm$ and is maintained independent on the dimming range that is between 90% and 10%. However, BER of 10^{-3}, requires only $P_{OFDM} = 12dBm$ and is maintained independent on the dimming range that is between 92% and 7%. Thus P_{OFDM} has to be optimized for maximum data-rate, minimum BER and/or target dimming range.

For a target BER of 10^{-3} and AWGN of -3dBm, Fig. 10 shows the possible modulation order as a function of the optical dimming as well as the perceived dimming. It is clearly noticed how a wide dimming range of operation is supported for example between 88% and 12% for optical

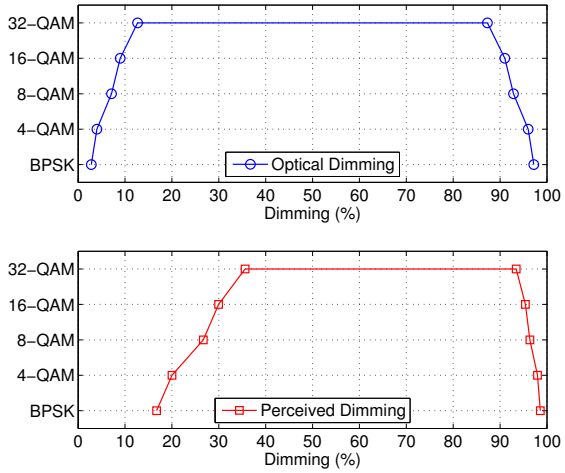

Figure 10: Modulation order vs. optical dimming (upper) and perceived dimming (lower).

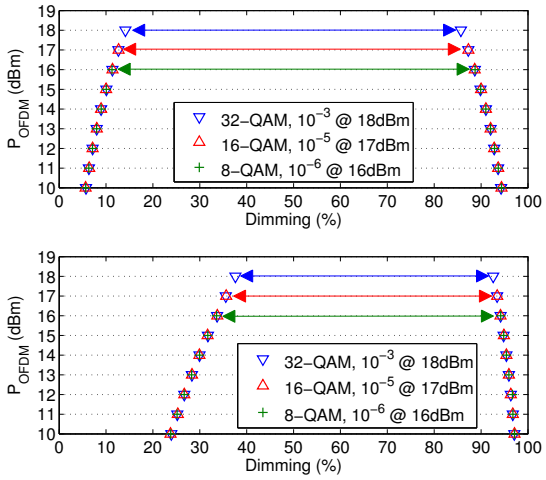

Figure 11: P_{OFDM} vs. optical dimming (upper) and perceived dimming (lower).

dimming and between 93% and 35% for perceived dimming, while maintaining 32-QAM. Beyond this range, 8-QAM, is maintained between 93% and 7% for optical dimming and between 97% and 26% for perceived dimming.

Finally, Fig. 11 clearly shows the corresponding dimming range at optimum values of P_{OFDM} for 8-QAM, 16-QAM, and 32-QAM. For example, using $P_{OFDM} = 18dBm$ jointly maximizes the spectral efficiency for 32-QAM and minimizes the BER. This BER is maintained independent on the dimming range that is between 87% and 14%. The dimming range can be extended by reducing P_{OFDM} (loss in BER) up to 1dB ($P_{OFDM} = 17dBm$) while maintaining $BER = 10^{-3}$. To further extend the dimming range, a switch to 16-QAM (loss in spectral efficiency) is required. Using 16-QAM, the dimming range can be further extended by reducing P_{OFDM} up to 3dB ($P_{OFDM} = 14dBm$) while maintaining BER below 10^{-3}. The corresponding values of D to obtain certain dimming set-points at different values of P_{OFDM} are shown in Fig. 7. Using Fig. 11 and Fig. 7

(having the same *x*-axis), for example, at optimum P_{OFDM}, $D = 8\%$ and $D = 12\%$ are required to obtain 20% optical dimming for 32-QAM and 16-QAM, respectively.

6 Conclusion

Our numerical simulations show that the proposed RPO-OFDM and dimming/communication signals combination algorithm demonstrate the viability of achieving both dimming and high data rate goals across a wide range of intensity settings while preserving compliance with industry-standard dimming techniques. High data rates promised by O-OFDM modulation can be maintained while offering a wide dimming range to serve illumination and/or energy saving goals. In RPO-OFDM, when a room is to be dimly lit, the communication capacity does not not need to be reduced proportional to intensity. The BER performance can be significantly improved because the proposed algorithm utilizes the full dynamic range of an LED and eliminates the need to adaptively adjust the LED operating point (DC bias) to maximize the dimming range while maintaining a good SNR to fulfill a target data rate. We anticipate describing implementation details of how the PWM and RPO-OFDM will be achieved in practical systems in future works.

References

[1] M. H. Crawford, "LEDs for solid-state lighting: performance challenges and recent advances," Selected Topics in Quantum Electronics, IEEE Journal of **15**(4), 1028–1040 (2009).

[2] C. DiLouie, *Advanced lighting controls: energy savings, productivity, technology and applications* (The Fairmont Press, Inc., 2006).

[3] E. F. Schubert, T. Gessmann, and J. K. Kim, *Light emitting diodes* (Wiley Online Library, 2005).

[4] H. Elgala, R. Mesleh, and H. Haas, "Indoor optical wireless communication: potential and state-of-the-art," Communications Magazine, IEEE **49**(9), 56–62 (2011).

[5] H. Elgala, R. Mesleh, and H. Haas, "Indoor broadcasting via white LEDs and OFDM," Consumer Electronics, IEEE Transactions on **55**(3), 1127–1134 (2009).

[6] M. B. Rahaim, A. M. Vegni, and T. D. Little, "A hybrid radio frequency and broadcast visible light communication system," in GC Wkshps, 792–796, (IEEE, 2011).

[7] H. Ma, L. Lampe, and S. Hranilovic, "Integration of indoor visible light and power line communication systems," in ISPLC, 291–296, (IEEE, 2013).

[8] H. Le Minh, Z. Ghassemlooy, D. O'Brien, and G. Faulkner, "Indoor gigabit optical wireless communications: challenges and possibilities," in ICTON, 1–6, (IEEE, 2010).

[9] J. Vucic and K.-D. Langer, "High-speed visible light communications: State-of-the-art," in OFC/NFOEC, 1–3, (IEEE, 2012).

[10] R. Mesleh, H. Elgala, and H. Haas, "Performance analysis of indoor OFDM optical wireless communication systems," in WCNC, 1005–1010, (IEEE, 2012).

[11] E. Pisek, S. Rajagopal, and S. Abu-Surra, "Gigabit rate mobile connectivity through visible light communication," in ICC, 3122–3127,(IEEE, 2012).

[12] P. Apse-Apsitis, A. Avotins, and L. Ribickis, "Wirelessly controlled LED lighting system," in ENERGYCON, 952–956, (IEEE, 2012).

[13] Z. Wang, W.-D. Zhong, C. Yu, J. Chen, C. P. S. Francois, and W. Chen, "Performance of dimming control scheme in visible light communication system," Optics Express **20**(17), 18861–18868 (2012).

[14] G. Ntogari, T. Kamalakis, J. Walewski, and T. Sphicopoulos, "Combining illumination dimming based on pulse-width modulation with visible-light communications based on discrete multitone," Journal of Optical Communications and Networking **3**(1), 56–65 (2011).

[15] Y. Gu, N. Narendran, T. Dong, and H. Wu, "Spectral and luminous efficacy change of high-power LEDs under different dimming methods," Proc. SPIE **6337**, 63370J–63370J-7 (2006).

[16] J. Armstrong and B. J. Schmidt, "Comparison of asymmetrically clipped optical OFDM and DC-biased optical OFDM in AWGN," Communications Letters, IEEE **12**(5), 343–345 (2008).

[17] N. Fernando, Y. Hong, and E. Viterbo, "Flip-OFDM for optical wireless communications," in ITW, 5–9, (IEEE, 2011).

[18] A. Nuwanpriya, A. Grant, S.-W. Ho, and L. Luo, "Position modulating OFDM for optical wireless communications," in GC Wkshps, 1219–1223, (IEEE, 2012).

[19] D. Tsonev, S. Sinanovic, and H. Haas, "Novel unipolar orthogonal frequency division multiplexing (U-OFDM) for optical wireless communication," in VTC-Spring, 1–5, (IEEE, 2012).